Measurements of atomic parameters of highly charged ions for interpreting astrophysical spectra

G. V. Brown[1], P. Beiersdorfer[1], K. R. Boyce[2], K. C. Gendreau[2], M. F. Gu[3], J. Gygax[4], S. M. Kahn[3], R. Kelley[2], F. S. Porter[2], D. W. Savin[3], and S. B. Utter[1]

[1]*Lawrence Livermore National Laboratory, Livermore, CA*

[2]*NASA Goddard Space Flight Center, Greenbelt, MD*

[3]*Columbia University, New York, NY*

[4]*Swales and Associates, Beltsville, MD*

Abstract

High-resolution x-ray spectra obtained by the *Chandra X-ray Observatory* and the *X-ray Multi-Mirror Mission* put new demands on atomic data including line positions, excitation cross sections, and radiative rates of cosmically-abundant highly-charged ions. To address this need, we are performing measurements of the line emission from ions of cosmically abundant elements. The data are obtained at the LLNL Electron Beam Ion Trap and focus on cross sections for electron-impact excitation, dielectronic recombination, and resonance excitation as well as atomic structure measurements. We find that ratios of the electron-impact excitation cross sections of singlet and triplet levels are systematically different from the calculated values in the case of many highly charged ions. This, for example, has a profound impact on inferring optical depths from solar and stellar atmospheres. Moreover, new line identifications are presented that resolve some long-standing puzzles in the interpretation of solar data, and the importance of resonance contributions to the spectral emission is assessed.

PACS:32.30 Rj–32.70.Fw–33.20.Rm–97.10.Ex–96.60.Tf

email: brown86@llnl.gov

I. INTRODUCTION

Highly-charged ions are present in a variety of non-terrestrial sources such as the corona of the Sun, stellar atmospheres, clusters of galaxies, and super-nova remnants. These sources have temperature components greater than 1 MK and thus produce high charge states of cosmically abundant elements such as Fe and Ni. The radiation produced by these ions is essentialy the only means of diagnosing the physical properties of these sources. A large portion of this radiation falls in the x-ray band below 20 Å, making this band is one of the most useful for inferring a source's physical conditions. Sounding rockets and satellites have observed this radiation with high resolution in the case of the Sun. Until recently, the x ray spectra of non-solar sources have typically been observed only with low resolution, with the emphasis being on the imaging and detection of sources. In the past year, however, the launch of the *Chandra X-Ray Observatory* (*CXO*) and the *X-Ray Multi-Mirror Mission* (*XMM*) has changed this situation drastically. Both these missions provide x-ray spectra of non-solar sources which rival and exceed those taken by the solar missions. These data have opened up the X-ray band as source of line diagnostics not before available to the astrophysics community (see Fig. 1).

The ability to reliably interpret the high-resolution spectra provided by *CXO* and *XMM* depends on a correct understanding and implementation of the atomic data on which the line emission is based. The more accurate and complete the data base of the relevant ions the higher chance that models will be able to reproduce the observations and to extract reasonable physical parameters. However, when it was not possible to fit the spectra from the *Advanced Satellite for Cosmology* and *Astrophysics* (*ASCA*) [1,2], which had a resolution of only about 100 eV, the atomic data came into question. It was found that the atomic parameters of cosmically abundant highly charged ions in the data bases do not meet a level of completeness and accuracy necessary to reproduce the observations. Attempts to fit high resolution solar data demostrated similar problems [3].

To provide accurate and complete atomic data of the relevant highly charged ions, a

laboratory astrophysics program has been established at the Lawrence Livermore National Laboratory (LLNL) Electron Beam Ion Trap (EBIT) experiment. This program provides laboratory measurements that include wavelengths, relative line intensities, and cross sections for collisional excitation, resonant excitation, and dielectronic recombination that are needed to model the line intensities of highly charged cosmically abundant ions. Unlike other laboratory sources, the LLNL EBIT has the advantage of operating in a density and energy regime relevant to astrophysical sources and with a high level of control found not achieved elsewhere. In the following, is a synopsis of some of our results.

II. THE LAWRENCE LIVERMORE NATIONAL LABORATORY'S ELECTRON BEAM ION TRAP

The first electron beam ion trap was designed and implemented at the Lawrence Livermore National Laboratory and was specifically developed and built for studying the interactions of electrons with highly charged ions using X-ray spectroscopy [4–6]. In brief, EBIT consists of a mono-energetic electron beam, an electrostatic trapping region in which ion–electron interactions take place, a collector where the beam is collected after interaction, and a metal vacuum vapor arc (MeVVA) used for injection of the target ions. The MeVVA produces singly or doubly ionized ions which are injected into the trap and further ionized to the desired charge state collisionally by the electron beam. Once trapped, the emitted radiation is measured via axial slots cut in to the drift tubes and aligned with vacuum ports permitting direct line of sight access to the trap. Typical operating energies range from 200–200,000 eV and densities from $2 \times 10^{11} - 5 \times 10^{12}$ cm^{-3}.

Over the past decade an ensemble of spectrometers have been developed and installed at the LLNL EBIT that cover the band width from 1–7000 Å with an emphasis on the x-ray and EUV regions. This includes von Hamos type curved crystal spectrometers providing K-shell spectra below 5 Å [7], two flat-crystal spectrometers operating *in vacuo* provide detailed L-shell and K-shell spectra in the 4 – 25 Å region [8], and two flat-field spectrometers, one

with a 1200 ℓ/mm, the other with 2400 ℓ/mm covering the 10 – 400 Å extreme ultraviolet region [9]. Recently, an X-ray calorimeter with parameters identical to those of the X-Ray Spectrometer (XRS) [10] that had been part of the *Astro-E* mission has been attached to the LLNL EBIT. This spectrometer has $\sim$ 10 eV resolution from 150 eV up to 10 keV. This signal is used in conjunction with the high-resolution crystal and grating spectrometers for cross section normalization and for monitoring the presence of impurity ions. Typical spectra measured with these spectrometers is given in Fig. 2.

The mono-energetic electron beam employed by EBIT makes it possible to isolate a particular charge state so that line emission can be positively identified with a particular ion. It also provides the means for studying specific population processes such as dielectronic recombination and resonance excitation. We have the ability to sweep the energy of the electron beam making it possible to study line population processes in an efficient manner. Plotting electron beam energy versus photon energy it is possible to evaluate where the resonances occur, and how relevant they are to the line flux.

Using the ability to sweep the electron beam energy in time has made it possible for us to simulate a Maxwellian temperature [11]. The beam is swept in a functional form such that when integrated over a sweep period the same electron energy distribution is found as in a Maxwellian distribution. In contrast to calculations of spectra at Mawellian temperatures, which require the correct synthesis of large sets of atomic parameters and processes and where some processes are invariably left out or incorrectly accounted for, the EBIT Maxwellian automatically includes all the processes which play a role in the line formation. The spectra in Fig. 2 were obtained by using this capability unique to our machine.

III. MEASUREMENT RESULTS

Owing to the fact that there have been several problems with the spectral package's ability to fit the portion of the observed spectra where the Fe L-shell line emission falls,

even in the low resolution data such as that from *ASCA*, we have directed our efforts to experimentally "map out" the radiation emitted from L-shell transitions in highly-charged iron ions. This "mapping" includes the wavelengths of the transitions, the relative intensities of the lines, the processes which populate each of the lines and even discerning the relevancy of the lines.

The first portion of our L-shell study involved the measurement and identification of all of the line emission from Fe XVII–XXIV falling in the 10–18 Å wavelength band [12,13]. This survey consists of lines populated by direct electron impact excitation from the ground state followed by radiative cascades. The results consist of 184 features across these seven charge states of iron, including the relative intensities. Of these 184 features, Phillips *et al.* [3] identify 133 in spectra form the corona of the sun, the MEKA model includes 90 [14], and the compilation of Kelly includes 102 [15]. Our list is, therefore, currently the most comprehensive. The deviations of those lines common to our list and these alternate sources are $\sim$ 15–20 mÅ for Fe XVII–Fe XXIV and $\approx$ 2–5 mÅ for Fe XXIV. Our survey is complete in the sense that all but very weak lines produced by direct impact excitation followed by radiative cascades at an electron density near 10^{12} cm^{-3} were observed and cataloged.

The wavelength survey provided a positive identification of the fluorine-like Fe XVIII line at 17.623 $\pm$ 0.003 Å. This line has been observed in several spectra of the solar corona and over the years its identification has been controversial. This line had been tentatively identified characteristic line by McKenzie *et al.* [16]; however, the laboratory value of 17.59 $\pm$ 0.02 Å for this characteristic line [17] is in disagreement with the wavelength McKenzie *et al.* [16] reported from the solar measurement. This measurement, together with the calculations by Cornille *et al.* [18] show that this line is emitted from the Fe XVIII ion. A complete explanation of this identification, including our measurement, can be found in Drake *et al.* [19].

The high-n transitions, where $4 \leq n \leq 11$, fall in the 10–11 Å wavelength band. The relative flux of the sum of all of these lines is 13% of the flux in the strongest Fe XVII line at 15.01 Å [12]. Because their contribution was believed to be insignificant, transitions

originating in levels with $n > 5$ had not been included in the spectral models. However, our measurements show that the high-n flux is significant and that its inclusion in the models could account for almost all of the discrepancy seen in the Capella spectrum [2].

The Fe XVII $^1P_1$ resonance line at 15.01 Å is the strongest L-shell line emitted from the Fe XVII ion. This line along with the $^3D_1$ intercombination line at 15.26 Å create a distinct feature seen in the spectrum of Fe XVII. For decades, these line features have been observed and well resolved by a multitude of experiments observing the Sun. When comparing the observed intensity ratio of these lines to more recent calulations, a large discrepancy is found. For example, the measured ratio from a sounding rocket experiment found a value of 2.05 $\pm$ 0.1 [20] while the recent calculation gave a value of 3.99 [21]. The discrepancy has been attributed to resonant scattering of the 3C line flux out of the line of sight [22,23]. Some authors have taken advantage of this scattering to infer physical parameters of the source such as optical depth and column density [24]. However, over the last few decades there has been several calculations of this line ratio with values ranging from 2.9 to 4.7. This large discrepancy makes it impossible to reliably infer the amount of scattering.

Using the measurement capabilities provided by the LLNL EBIT, this ratio has been measured under conditions where various population processes may contribute to the flux of either line in the optically thin limit where no scattering occurs. The results of these measurements demonstrates that the ratio for the steady state case above threshold is 3.04 $\pm$ 0.04 and that all of the values measured under all the conditions fall within 10% (see Fig. 3). The lower values are 2.77 $\pm$ 0.19 which was measured at a single electron beam energy just above the threshold so that no cascades can contribute to either line, and 2.79 $\pm$ 0.15 measured in the presence of sodium-like innershell satellites which blend with the 3D line. Measurements which inlcude Na-like innershell satelites were made when the relative population of sodium to neon like ion abundance was $\sim$ 10% and hence a larger sodium like abundance would further reduce the line ratio. Comparing our values to those measured in the Sun shows that in many cases there is good agreement and it is, therefore, not necessary to invoke the idea of resonant scattering. In some cases, however, the solar ratio is much

lower than our measured values (see Fig. 3). For example, Waljewski *et al.* quote a ratio of 1.87 $\pm$ 0.21. This value was measured from a non-flaring active region of the sun, while those that agree with our measurements were during a flare. Because the Na-like abundance is considerably higher in the cooler non-flaring region, the blending of Na-like innershell satellites was identified by our measurements as a likely reason behind the reduced ratio.

Energy dependent measurements of the electron-ion interaction processes have been carried out for many ions between Fe VII and Fe XXVI in the EUV and X-ray region. For example, the Fe XXIV corresponding to the transitions $3d_{5/2} \rightarrow 2p_{3/2}$, $3p_{1/2} \rightarrow 2s_{1/2}$, and $3p_{3/2} \rightarrow 2s_{1/2}$ have been studied [25]and compared to detailed R-matrix and distroted-wave calculations of Berrington and Tully [26] and Zhang *et al.* [27] (see Fig. 4). These measurements show that for a collisionally ionized plasma at temperatures where the ion abundance peaks, the DR contribution to the line emission is $\leq$ 10% and the resonance excitation contribution is $\leq$ 5%.

IV. SUMMARY

The insufficiencies of the atomic data in spectral models used to fit astrophysical data demonstrate the need for laboratory astrophysics. Accurate and complete sets of atomic data are necessary to take full advantage of the high-resolution spectral data being provided by *CXO* and *XMM*. An ensemble of spectrometers and operating conditions have been developed and used at the LLNL EBIT providing data to meet this need. We have already provided complete set of wavelengths and relative line intensites for all of the L-shell line emission falling in the 10–18 Å wavelength band demonstrating that the list used in the present models are incomplete, we have a definitive relative intensity for the resonant and intercombination line in Fe XVII in the optically thin limit demonstrating that it is not necessary to invoke the idea of resonant scattering, and we have shown examples of line excitation functions which demonstrate the need for inclusion of DR and RE in atomic models. With the recent installation of the x-ray calorimeter we are now able to measure absolute

cross sections relative to the radiative recombination cross section for the L-shell line emission. As a whole, the laboratory data provided by the LLNL EBIT, which include reliable uncertainty limits, make it possible to establish the level to which physical parameters can be inferred from astrophysical spectra.

We would like to thank M. Chen and K. Reed for their calculations and E. Magee and D. Nelson for their technical support. This work was performed under the auspices of the U. S. Department of Energy by the University of California Lawrence Livermore National Laboratory under contract No. W-7405-Eng-48 and was supported by the NASA High-Energy Astrophysics Supporting Research and Technology Program work order W-19127.

---

[1] A. C. Fabian, K. A. Arnaud, M. W. Bautz, and Y. Tawara, Astrophys. J. **436**, L63 (1994).

[2] N. S. Brickhouse et al., Astrophys. J. **530**, 387 (2000).

[3] K. J. H. Phillips et al., Astron. Astrophys. **138**, 381 (1999).

[4] R. E. Marrs, *Atomic, Molecular, and Optical Physics: charged particles*, volume 29A of *Experimental Methods in the Physical Sciences*, Academic Press, Inc., San Diego, CA, 1995, Chapter 14. Electron Beam Ion Traps.

[5] R. Marrs, P. Beiersdorfer, and D. Schneider, Phys. Today **47**, 27 (1994).

[6] M. Levine, R. Marrs, D. Knapp, and M. Schneider, Phys. Scr. **T22**, 157 (1988).

[7] P. Beiersdorfer et al., Rev. Sci. Instrum. **61**, 2338 (1990).

[8] G. V. Brown, P. Beiersdorfer, and K. Widmann, Rev. Sci. Instrum. **70**, 280 (1999).

[9] P. Beiersdorfer, J. C. López-Urrutia, J. R. C. Springer, S. B. Utter, and K. Wong, Rev. Sci. Instrum. **70**, 276 (1999)..

[10] R. Kelley et al., The *Astro-E* high resolution x-ray spectrometer, in *EUV, X-ray and Gamma-*

Ray Instrumentation for Astronomy X, volume 7, page 3765, Denver, 1999, SPIE.

[11] D. W. Savin et al., Phys. Scr. **T80**, 312 (1999).

[12] G. V. Brown et al., Astrophys. J. **502**, 1015 (1998).

[13] G. V. Brown, P. Beiersdorfer, D. A. Liedahl, S. M. Kahn, and K. Widmann. LLNL preprint UCRL-JC-136647.

[14] R. Mewe, E. H. B. M. Gronenschild, and G. H. J. van den Oord, Astron. Astrophys. Supp. **62**, 197 (1985).

[15] R. R. Kelly, J. Phys. Chem. Ref. Data **16**, 861 (1987), Supplement Series.

[16] D. L. McKenzie, P. B. Landecker, R. M. Broussard, H. R. Rugge, and R. M. Young, Astrophys. J. **241**, 409 (1980).

[17] J. Bearden, Rev. Mod. Phys. **39**, 78 (1967).

[18] M. Cornille, J. Dubau, M. Loulergue, F. Bely-Dubau, and P. Faucher, Astron. Astrophys. **259**, 669 (1992).

[19] J. J. Drake, D. A. Swartz, P. Beiersdorfer, G. V. Brown, and S. M. Kahn, Astrophys. J. **521**, 839 (1999).

[20] J. H. Parkinson, Solar Physics **42**, 183 (1975).

[21] M. Mohan, R. Sharma, and W. Eissner, Astrophys. J. **108**, 389 (1997).

[22] H. R. Rugge and D. L. McKenzie, Astrophys. J. **297**, 338 (1985).

[23] J. T. Schmelz, J. L. R. Saba, and K. T. Strong, Astrophys. J. Lett. **398**, L115 (1992).

[24] K. Waljeski et al., Astrophys. J. **429**, 909 (1994).

[25] M. F. Gu et al., Astrophys. J. **518**, 1002 (1999).

[26] K. A. Berrington and J. A. Tully, **126**, 105 (1997).

[27] H. Zhang, D. Sampson, and R. E. H. Clark, At. Data Nucl. Data Tables **44**.

Figure 1. Spectrum taken by SMM of a non-flaring active region of the Sun (a) compared to a spectrum taken by CXO of Capella. This figure demonstrates the high resolution spectra available for both solar and extra-solar sources.

Figure 2. Spectrum of the iron L-shell emission recorded (a) by the high-resolution x-ray calorimeter and (B) by one of the four availabe flat-crystal spectrometers. The measurements were carried out at an electron temperature of 0.9 and 0.6 keV, respectively.

Figure 3. Results of measurements of the intensity ratio fo the 3C to 3D line located at 15.01 and 15.26 Å, respectively. The range of the EBIT results includes all processes such as Na-like DR satellites and innershell excitation are included among the measured values. The calculations consist of collision strengths, cross sections and, rate coefficients. The EBIT band falls below nearly all of the calculated values. There is , however, agreement between the EBIT values and the values from flaring active regions[†] of the Sun. The low ratios measured in the non-flaring active regions may be the result of blending with Na-like Fe XVI innershell satellites.

Figure 4. Cross sections for producing Fe XXIV line emission. The solid lines are the R-matrix calculations of DE and RE plus HULLAC calculations for $n \leq 7$ cascades contributions. The dotted lines are the DW calculations of Zhang *et al.* plus HULLAC calculations for cascades. The dashed lines are HULLAC calculations. Circles are the experimental results normalized to the resonance-free energies between 2.0 and 3.0 keV. The line emission below threshold is due to DR satellites.

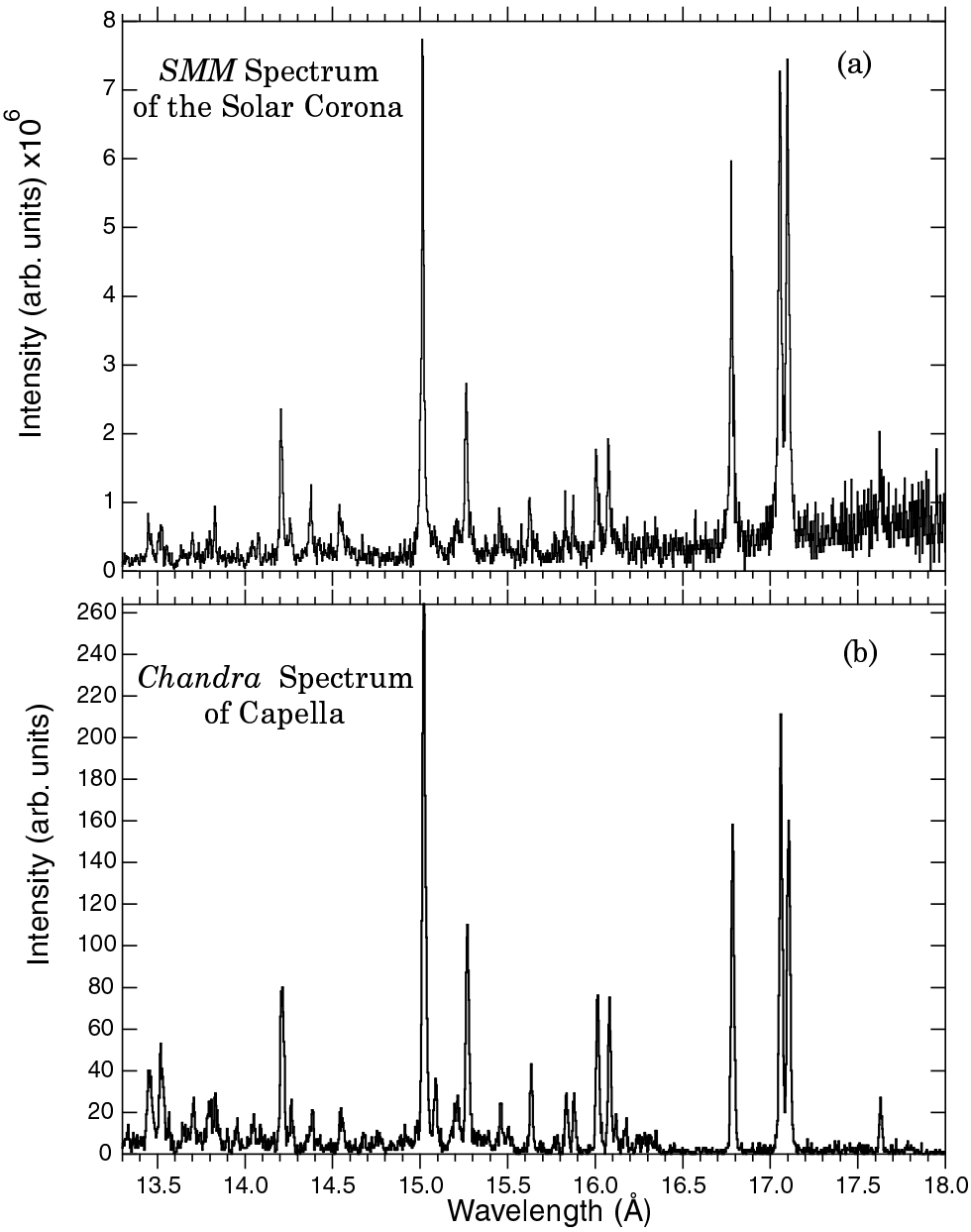

Flg.1.

FIG. 1. Spectrum taken by SMM of a non-flaring active region of the Sun (a) compared to a spectrum taken by CXO of Capella. This figure demonstrates the high resolution spectra available for both solar and extra-solar sources.

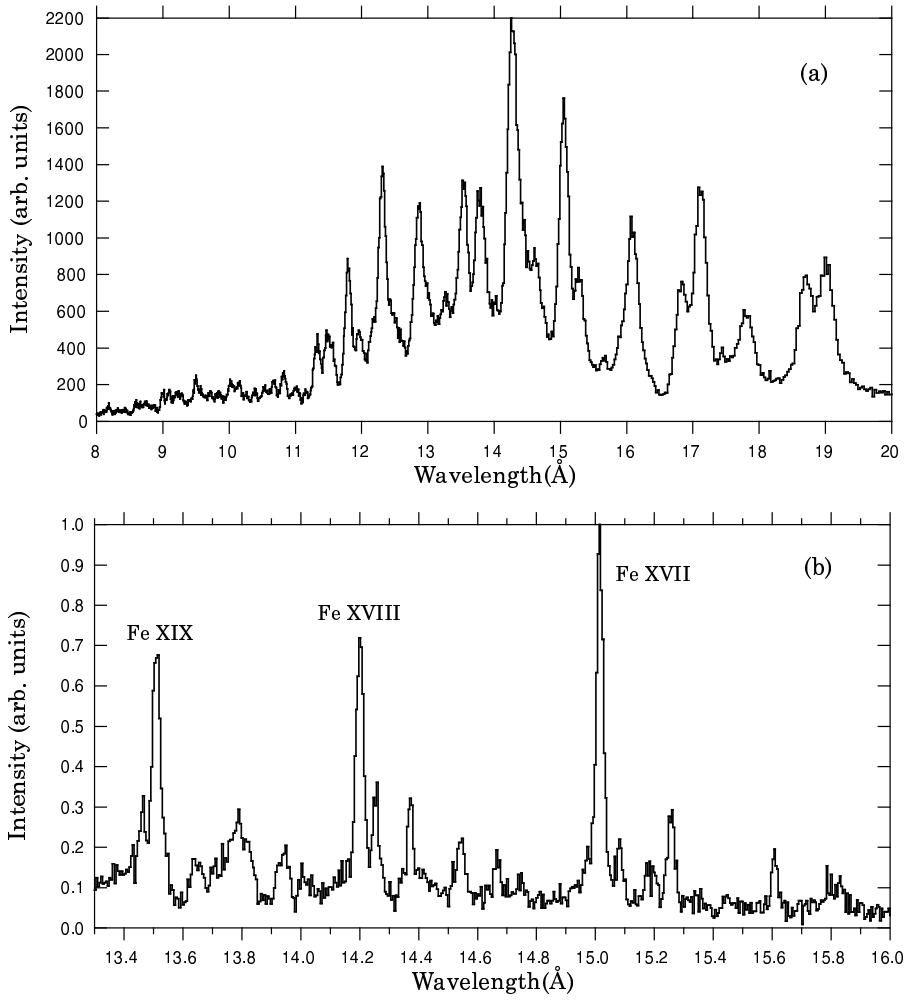

Fig. 2.

FIG. 2. Spectrum of the iron L-shell emission recorded (a) by the high-resolution x-ray calorimeter and (B) by one of the four availabe flat-crystal spectrometers. The measurements were carried out at an electron temperature of 0.9 and 0.6 keV, respectively.

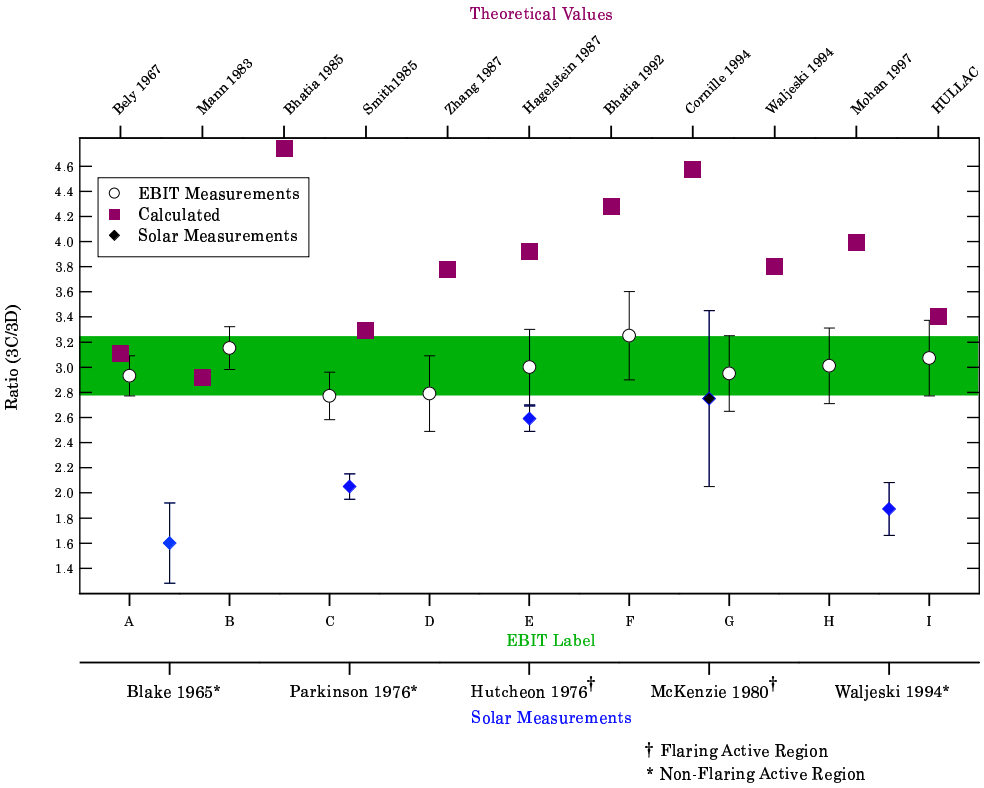

Fig.3.

FIG. 3. Results of measurements of the intensity ratio fo the 3C to 3D line located at 15.01 and 15.26 Å, respectively. The range of the EBIT results includes all processes such as Na-like DR satellites and innershell excitation are included among the measured values. The calculations consist of collision strengths, cross sections and, rate coefficients. The EBIT band falls below nearly all of the calculated values. There is , however, agreement between the EBIT values and the values from flaring active regions† of the Sun. The low ratios measured in the non-flaring active regions may be the result of blending with Na-like Fe XVI innershell satellites.

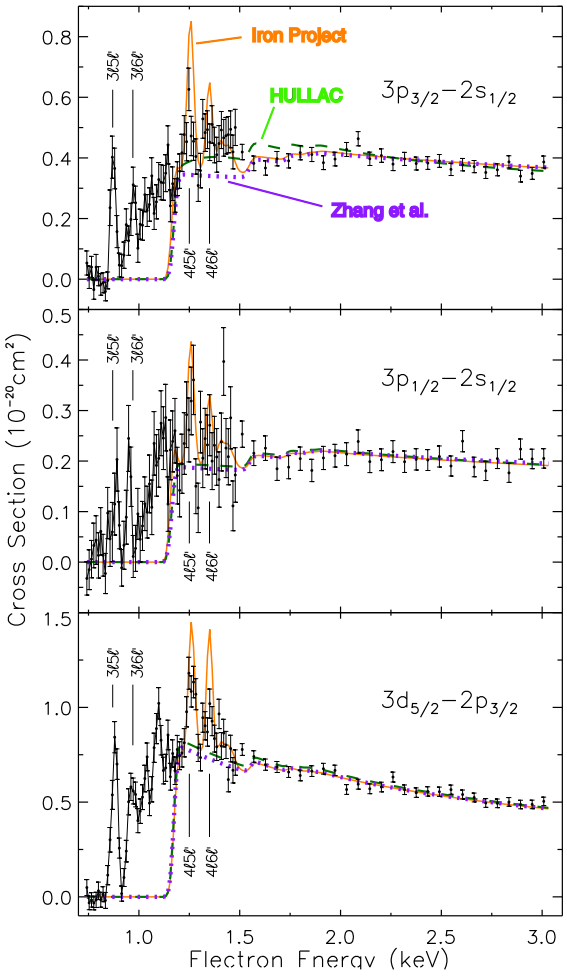

Fig.4.

FIG. 4. Cross sections for producing Fe XXIV line emission. The solid lines are the R-matrix calculations of DE and RE plus HULLAC calculations for $n \leq 7$ cascades contributions. The dotted lines are the DW calculations of Zhang *et al.* plus HULLAC calculations for cascades. The dashed lines are HULLAC calculations. Circles are the experimental results normalized to the resonance-free energies between 2.0 and 3.0 keV. The line emission below threshold is due to DR satellites.